ALTERATION OF CHROMATIN STRUCTURE DURING LPS TOLERANCE ACQUISITION IN *Salmonella enterica*-INFECTED MACROPHAGES

A PREPRINT

Cyril Matthey-Doret[1,2], ...

September 7, 2021

1 Institut Pasteur, Spatial Regulation of Genomes unit, CNRS, UMR 3525, C3BI USR 3756, Paris, France
2 Sorbonne Université, Collège Doctoral, F-75005 Paris, France
3 ...

ABSTRACT

***K*eywords** Genomics · Hi-C · Host-parasite

1 Introduction

Salmonella is an intracellular bacterium and human pathogen causing an enteric disease known as salmonellosis in many animals. It is usually contracted by ingestion of contaminated foods or water and infiltrates the intestinal epithelium. Salmonella destabilizes tight junctions between epithelial cells, favoring the migration of neutrophils through the epithelial layer by stimulating the mitogen-activated protein kinase (MAPK) and NF-κB pathways [1, 2]. The sensing of bacterial lipopolysaccharides (LPS) present on the bacterial cell surface through Toll-like receptors (TLR) elicits the production of interleukins and activation of caspase genes [3] which further increase intestinal inflammation.

Salmonella can then infect many cell types in the epithelium including macrophages [4]. Upon cell entry, Salmonella secretes effector proteins through its type III secretion system to manipulate the host defenses and metabolism, and replicate inside the cell. A combination of replicating and non-replicating bacteria can co-exist within the host cell [5]. Non-replicating cells - also called persisters - have increased antibiotic resistance and are of particular concern for the treatment of salmonellosis [6].

In response to bacterial infection, host macrophages secrete chemokines and cytokines to recruit other immune cells to the infection site. They also produce reactive oxygen species and microbicidal molecules to kill surrounding bacterial cells. This response is stimulated by LPS present on the cell surface of gram-negative bacteria such as *Salmonella*. However, in cases of prolonged exposure, this can lead to an overstimulation of the immune system which can lead to endotoxic shock and poses the threat of tissue damage, organ failure and death. To avoid such outcome, the body can enter a transient state of hyporesponsiveness to infection known as endotoxin-tolerance, or LPS-tolerance. During this period, macrophages are reprogrammed to cease production of inflammatory molecules and instead focus on tasks such as tissue repair and phagocytosis of cellular debris.

A complex interplay takes place between host inflammatory factors and bacterial effectors. Upon invasion of the intestinal lumen by *Salmonella*, the release of ROS by macrophages leads to a growth advantage for the pathogen over resident bacteria from the microbiome [7]. Conversely, after cellular entry *Salmonella* effectors dampen inflammation to favor intracellular survival, reducing IL-8 secretion and MAPK-mediated inflammation using its effector proteins [8]. This suggests that *Salmonella* will increase and decrease inflammatory response at different stages of infection.

Understanding how bacteria manipulate the host immune response is an important step towards treating and mitigating risks associated with Salmonella infection. Many levels or regulation are affected by the bacterium, including signal transduction pathways [9], mitochondrial metabolism [10], RNA splicing [11] and histone marks [12].

In mammals, gene regulation is intertwined with genome compaction and folding. At the broadest level, chromatin is segregated into active and inactive compartments, which can change according to the needs of the cell [13]. The genome is also partitioned into Topologically Associating Domains (TADs) which can form insulated neighbourhood of co-regulated genes [14]. Regulatory interactions are also mediated by chromatin loops which can modulate gene activity by putting them in physical contact with enhancers or promoters. In mammals, these chromatin structures are mainly orchestrated by the CCTC-binding factor (CTCF) [15]. CTCF-mediated loops are thought to play roles in immunity, such as increasing the expression of genes in the major histocompatibility complex (MHC) locus [16, 17, 18], or coordinating the expression of interleukins [19, 20]. The LPS-tolerance phenomenon is thought to be regulated by epigenetic mechanisms such as histone modifications [21, 22, 23], but thus far the implication of genome conformation in that state has not been investigated.

Here we investigate the consequences of Salmonella infection on the genome structure of mammalian host cells. Using Hi-C in Mouse bone marrow macrophages (BMM), we measure spatial genomic features at early and late Salmonella infection and how they relate to gene deregulation. We find genome-wide changes in chromatin compartments and overall organization during late infection (around 20h post infection). This coincides with the time at which LPS (Lipopolysaccharide) tolerance is acquired, a transient period of hyporesponsiveness, during which cells become desensitized to bacterial presence to prevent over-activation of the immune response and self-damage [24]. We find that chromatin loops changes are enriched in genes related to histone modifications, Rho GTPases and transcriptional regulation and we identify several key markers of LPS tolerance associated with long range interactions during infection.

2 Results

We used Hi-C to capture chromosome conformation of murine BMM infected by Salmonella as well as bystander cells exposed to salmonella was measured in uninfected cells and at two timepoints representing early (1h) and late (20h) infection. We also used a secretion system SsaV mutant *Salmonella* to assess whether chromatin structure was associated with secretion of effector proteins. We used 3 different Hi-C derived features to measure chromosome structural changes: The stratum-adjusted correlation coefficient [25], which measures overall contact simiarity between Hi-C matrices of sample pairs (Fig. 1a), the slope of the distance-contacts decay function (Fig. 1b), which reflects chromatin compaction along the genome, and A/B compartment eigenvectors (Fig. 1c), which compares the segmentation of the genome into active and inactive chromatin. We found that most changes happened during late (20h) infection, regardless of Salmonella genotype or bystander versus infected status. Infection timepoint (20h vs 2h) was the main determinant with respect to all 3 aforementioned features.

The time at which we observe strongest conformational changes coincide with the time range for the acquisition of LPS tolerance (16 - 48h) [26]. To focus on such changes, we resequenced Hi-C libraries from samples infected by WT Salmonella at those timepoint (each time point in duplicates). This allowed us to inspect changes in fine grained chromatin structures, such as chromatin loops and borders.

We used Hi-C to measure compartment changes at two time points in infected cells. Genome-wide A/B compartmentalization was stronger at late infection (Fig. 1d) compared to early infection or uninfected cells. We use CHESSas a slight increase in chromatin loops intensity. These large scale changes are could be attributed to physiological changes in late infection. In particular, the shift to active compartment together with increased domain border strength is likely due to active transcription changes at highly transcribed genes.

We ran gene set enrichment analysis (GSEA) separately on 4 differential features during late infectino (20h vs 2h): A/B compartment, chromatin loops, domain borders and gene expression. After multiple testing correction (Benjamini Hochberg, FDR rate=0.1), all 4 features are enriched in pathways related to leukocyte chemotaxis and migration. To further explore the relationship between those features, we generated a graph using enrichment map [28] to visualize the overlap between GO terms and the relationship between structural features and gene expression (methods). The largest component of this graph contains GO terms related to chemotaxis and migration, as well as other pathways (Fig. 3a). Chromatin features are limited to certain modules of that graph, while gene expression is dysregulated in most nodes.

The genes responsible for structural and expression changes pertaining to chemotaxis mostly belong to a cluster of chemokine ligand (CXCL) genes (Fig. 3b). These genes produce small cytokines controling the migration and adhesion of monocytes.

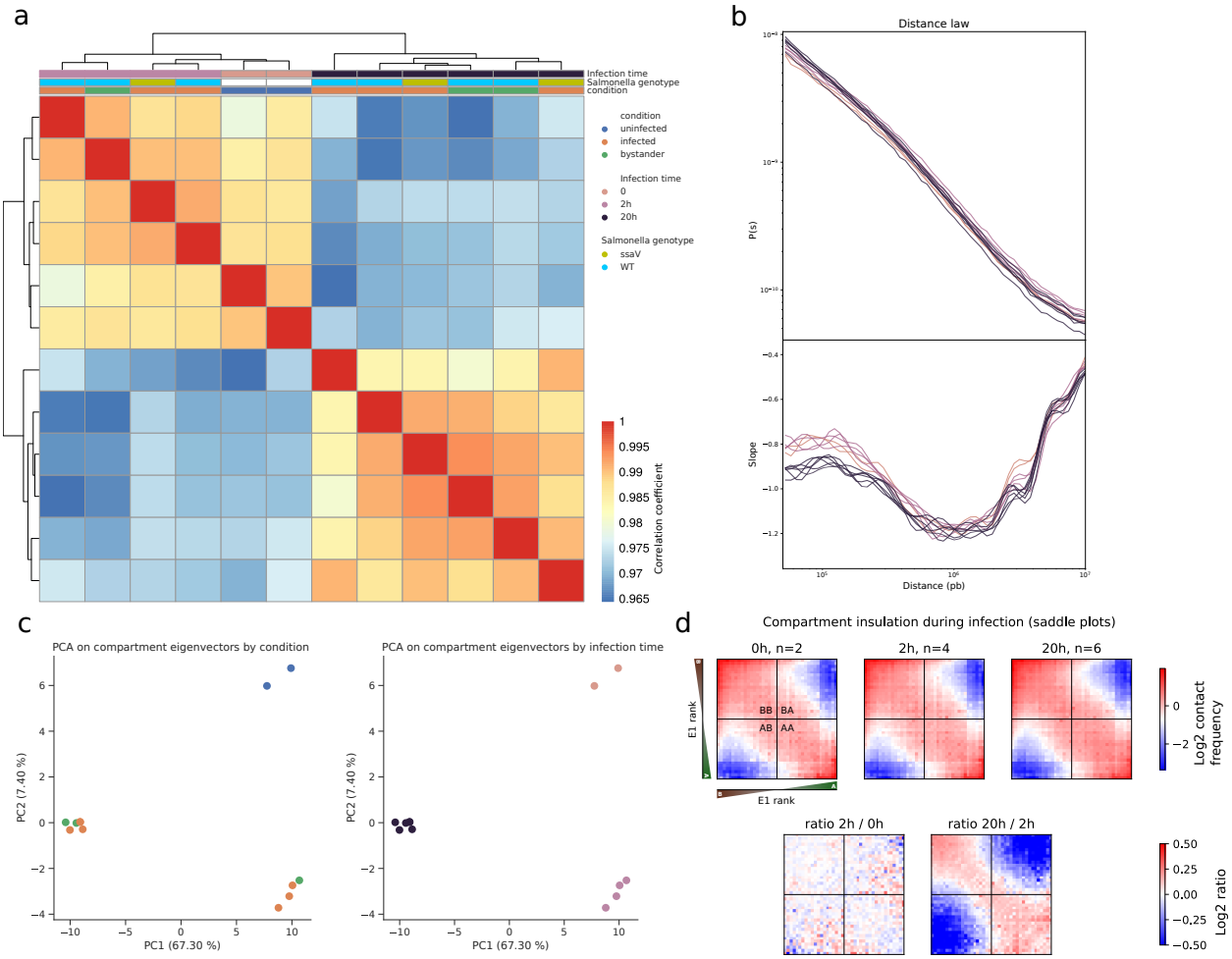

Figure 1: Global changes in genome conformation happen during late Salmonella infection. **a,** Heatmap of HiCRep stratum adjusted correlation coefficients between all pairs of samples. **b,** Distance-dependent contact decay (top) and its slope (bottom) according to infection time. **c,** PCA of chromatin compartment vectors with samples colored by condition (top) and infection time (bottom). **d,** Saddle plots showing compartment intensities during infection. Hi-C interactions are ranked according to their rank on the compartment eigenvector (E1) and discretized into quantiles. Saddle plots show the intensity of interactions between each pair of eigenvector quantile (top) and their change during infection (bottom) using the Log ratio of saddles between different time points.

2.1 Increase of chromatin looping at IL-10 locus

The anti-inflammatory cytokin interleukin 10 (IL-10) downregulates the inflammatory response to prevent damage to the host. Its expression is regulated by CTCF [19], and it is thought that chromatin looping coordinates the gene expression in that locus [19]. We found increase in chromatin loop strength during late infection, further supporting the role of CTCF looping in interleukin regulation.

The position of chromatin loops anchors were refined using ATAC-seq differential peaks and classified based on their location (TSS, TTS, inter-gene, intronic, exonic). This classification was further expanded using epigenetic marks to include enhancer, promoter and repressed (Methods). Among loops overlapping differential ATAC-seq peaks, there were 36 loops anchored at the promoters of differentially expressed genes, including genes related to cell adhesion and cytoskeleton (ACTN1, ICAM5, P2RX4, TGFB1).

We also investigated the presence of complex infection-dependent loops, involving more than 3 partners. We found 13 such loops, several of which comprise genes related to the dampening of immune response and cytoskeleton.

3 Discussion

- Most 3D genome changes happen at late infection
- Coincide with LPS tolerance time
- 3D features enriched in chemotaxis and cell migration: LPS -> M2 Macrophages -> more motile [29]
- MHC compartment changes, consistent with previous microscopy observations of chromatin changes associated with transcription at MHC [30]
- Speed of structural changes more adapted to long term (LPS) than early response ?
- 3D often correlated with histone marks, so makes sense given that LPS is associated with histone deacetylation.

Methods

Libraries preparation

Hi-C library preparation

We used the Arima kit and followed manufacturer's instructions.

ATACseq library preparation

RNAseq library preparation

Analyses

All analyses were done using the mm10 reference assembly.

Differential accessibility peaks

ATACseq data was processed using the nf-core/atacseq pipeline (v1.2.1). Within nfcore/atacseq, consensus peaks were obtained using MACS2 and differential peaks from DESeq2 with FDR<0.05 were selected.

Histone marks ChIPseq

Publicly available histone mark ChIPseq datasets were retrieved from ENCODE and processed using the nf-core/chipseq pipeline (v1.2.1) in single-end mode. The following marks and respective accession numbers were used: H3K4Me1 (ENCSR000CFE), H3K4Me2 (SRR930721, SRR930722), H3K4Me3 (ENCSR000CFF), H3K27Me3 (SRR930746), H3K27Ac (ENCSR000CFD).

Differential expression

Libraries were aligned using Hisat2 and transcripts were quantified into TPM using salmon. Differential expression was measured between 2h and 20h p.i. using DESeq2.

Hi-C analyses

Hi-C matrices were generated using hicstuff (v3.0.1) [31]. Matrix balancing (normalization) was performed using the Cooler implementation of the ICE algorithmm [32] Compartments were extracted using the cooltools API [33].

Reproducibility between replicates was assessed using the hicreppy implementation (`https://github.com/cmdoret/hicreppy`)of the HiCrep algorithm [25].

Chromatin loops and domain borders were detected using chromosight [34] (v1.5.1) and pattern intensity changes between conditions were computed using pareidolia (v.0.6.0) [35]. Compartment detection was performed using cooltools (v0.3.2) [33] using gene density to orient eigenvectors. Hi-C matrices were binned at 320kb for compartment detection and Hi-C rep and 10kb for all other analyses.

Each gene was assigned the closest loop anchor and domain border within 200kb (if any). CHESS was used to identify genes with major structural changes during infection.

Gene set enrichment analysis

GSEA was performed using the python package gseapy [36]. The analysis was run 4 times independently on different phenotypes representing changes between 2h and 20h p.i. The phenotype used were: pareidolia differential pattern scores (loop and borders), compartment eigenvector differences from cooltools, and gene expression log2 fold change from DeSeq2. For structural phenotypes, values were assigned to genes using bedtools genome arithmetic operations [37]: Borders and loops were assigned to the closest gene within 200kb, and compartment values were assigned to genes using bedtools intersect.

For visualizing the graph, the union of all terms with p-values below 0.05 (without multiple testing correction) for all phenotypes was used. The graph was generated using cytoscape with the enrichmentMap plugin [28]. Nodes were colored by dataset (i.e. where the phenotypes' p-values are below 0.05) for visualization.

Integration of epigenomic data

Chromatin loops were intersected with differential ATAC peaks to retain only loops with both anchors within 10kb (a margin of 1 pixel on the Hi-C contact map) of differentially accessible ATAC peaks (FDR <0.05). Average normalized histone mark intensity scores were assigned to each peak and K-means clustering (k=3) was used on those intensities to classify anchors into 3 groups: promoter (highest H3K4Me3), enhancer (highest H3K4Me1) or low activity (other peaks). Peaks were histone marks were not available were labelled "unknown". Promoter anchors were further refined to include only those located in promoter regions (-1kb to +100bp from TSS).

Code availability

All codes to reproduce analyses is available on a Github repository at `https://github.com/cmdoret/mouse_salmonella_infection.git` where data processing is packaged into a Snakemake pipeline, and downstream analyses are provided as jupyter notebooks.

References

[1] B A McCormick, S I Miller, D Carnes, and J L Madara. Transepithelial signaling to neutrophils by salmonellae: A novel virulence mechanism for gastroenteritis. *Infection and Immunity*, 63(6):2302–2309, June 1995.

[2] B A McCormick, P M Hofman, J Kim, D K Carnes, S I Miller, and J L Madara. Surface attachment of Salmonella typhimurium to intestinal epithelia imprints the subepithelial matrix with gradients chemotactic for neutrophils. *Journal of Cell Biology*, 131(6):1599–1608, December 1995.

[3] Nicholas Arpaia, Jernej Godec, Laura Lau, Kelsey E. Sivick, Laura M. McLaughlin, Marcus B. Jones, Tatiana Dracheva, Scott N. Peterson, Denise M. Monack, and Gregory M. Barton. TLR Signaling Is Required for Salmonella typhimurium Virulence. *Cell*, 144(5):675–688, March 2011.

[4] M Martínez-Moya, M. A de Pedro, H Schwarz, and F García-del Portillo. Inhibition of Salmonella intracellular proliferation by non-phagocytic eucaryotic cells. *Research in Microbiology*, 149(5):309–318, May 1998.

[5] K. Z. Abshire and F. C. Neidhardt. Growth rate paradox of Salmonella typhimurium within host macrophages. *Journal of Bacteriology*, 175(12):3744–3748, June 1993.

[6] Daphne A. C. Stapels, Peter W. S. Hill, Alexander J. Westermann, Robert A. Fisher, Teresa L. Thurston, Antoine-Emmanuel Saliba, Isabelle Blommestein, Jörg Vogel, and Sophie Helaine. Salmonella persisters undermine host immune defenses during antibiotic treatment. *Science*, 362(6419):1156–1160, December 2018.

[7] Sebastian E. Winter, Parameth Thiennimitr, Maria G. Winter, Brian P. Butler, Douglas L. Huseby, Robert W. Crawford, Joseph M. Russell, Charles L. Bevins, L. Garry Adams, Renée M. Tsolis, John R. Roth, and Andreas J. Bäumler. Gut inflammation provides a respiratory electron acceptor for Salmonella. *Nature*, 467(7314):426–429, September 2010.

[8] Sumati Murli, Robert O. Watson, and Jorge E. Galán. Role of tyrosine kinases and the tyrosine phosphatase SptP in the interaction of Salmonella with host cells. *Cellular Microbiology*, 3(12):795–810, 2001.

[9] Doris L. LaRock, Anu Chaudhary, and Samuel I. Miller. Salmonellae interactions with host processes. *Nature Reviews Microbiology*, 13(4):191–205, April 2015.

[10] Haihua Ruan, Zhen Zhang, Li Tian, Suying Wang, Shuangyan Hu, and Jian-Jun Qiao. The Salmonella effector SopB prevents ROS-induced apoptosis of epithelial cells by retarding TRAF6 recruitment to mitochondria. *Biochemical and Biophysical Research Communications*, 478(2):618–623, September 2016.

[11] Athma A. Pai, Golshid Baharian, Ariane Pagé Sabourin, Jessica F. Brinkworth, Yohann Nédélec, Joseph W. Foley, Jean-Christophe Grenier, Katherine J. Siddle, Anne Dumaine, Vania Yotova, Zachary P. Johnson, Robert E. Lanford, Christopher B. Burge, and Luis B. Barreiro. Widespread Shortening of 3' Untranslated Regions and Increased Exon Inclusion Are Evolutionarily Conserved Features of Innate Immune Responses to Infection. *PLOS Genetics*, 12(9):e1006338, September 2016.

[12] Marcelo B. Sztein, Andrea C. Bafford, and Rosângela Salerno-Goncalves. Salmonella enterica serovar Typhi exposure elicits ex vivo cell-type-specific epigenetic changes in human gut cells. *Scientific Reports*, 10(1):13581, August 2020.

[13] E. Lieberman-Aiden, N. L. van Berkum, L. Williams, M. Imakaev, T. Ragoczy, A. Telling, I. Amit, B. R. Lajoie, P. J. Sabo, M. O. Dorschner, R. Sandstrom, B. Bernstein, M. A. Bender, M. Groudine, A. Gnirke, J. Stamatoyannopoulos, L. A. Mirny, E. S. Lander, and J. Dekker. Comprehensive Mapping of Long-Range Interactions Reveals Folding Principles of the Human Genome. *Science*, 326(5950):289–293, October 2009.

[14] Elphège P. Nora, Bryan R. Lajoie, Edda G. Schulz, Luca Giorgetti, Ikuhiro Okamoto, Nicolas Servant, Tristan Piolot, Nynke L. van Berkum, Johannes Meisig, John Sedat, Joost Gribnau, Emmanuel Barillot, Nils Blüthgen, Job Dekker, and Edith Heard. Spatial partitioning of the regulatory landscape of the X-inactivation centre. *Nature*, 485(7398):381–385, May 2012.

[15] Diego Ottaviani, Elliott Lever, Shihong Mao, Rossitza Christova, Babatunji W. Ogunkolade, Tania A. Jones, Jaroslaw Szary, Johan Aarum, Muhammad A. Mumin, Christopher A. Pieri, Stephen A. Krawetz, and Denise Sheer. CTCF binds to sites in the major histocompatibility complex that are rapidly reconfigured in response to interferon-gamma. *Nucleic Acids Research*, 40(12):5262–5270, July 2012.

[16] Rossitza Christova, Tania Jones, Pei-Jun Wu, Andreas Bolzer, Ana P. Costa-Pereira, Diane Watling, Ian M. Kerr, and Denise Sheer. P-STAT1 mediates higher-order chromatin remodelling of the human MHC in response to IFNγ. *Journal of Cell Science*, 120(18):3262–3270, September 2007.

[17] Parimal Majumder, Jorge A. Gomez, Brian P. Chadwick, and Jeremy M. Boss. The insulator factor CTCF controls MHC class II gene expression and is required for the formation of long-distance chromatin interactions. *The Journal of Experimental Medicine*, 205(4):785–798, April 2008.

[18] Parimal Majumder and Jeremy M. Boss. Cohesin regulates major histocompatibility complex class II genes through interactions with MHC-II insulators. *Journal of immunology (Baltimore, Md. : 1950)*, 187(8):4236–4244, October 2011.

[19] Tatjana Nikolic, Dowty Movita, Margaretha EH Lambers, Claudia Ribeiro de Almeida, Paula Biesta, Kim Kreefft, Marjolein JW de Bruijn, Ingrid Bergen, Niels Galjart, Andre Boonstra, and Rudi Hendriks. The DNA-binding factor Ctcf critically controls gene expression in macrophages. *Cellular & Molecular Immunology*, 11(1):58–70, January 2014.

[20] Shutao Cai, Charles C. Lee, and Terumi Kohwi-Shigematsu. SATB1 packages densely looped, transcriptionally active chromatin for coordinated expression of cytokine genes. *Nature Genetics*, 38(11):1278–1288, November 2006.

[21] Mohamed El Gazzar, Barbara K. Yoza, Jean Y. Q. Hu, Sue L. Cousart, and Charles E. McCall. Epigenetic Silencing of Tumor Necrosis Factor α during Endotoxin Tolerance*. *Journal of Biological Chemistry*, 282(37):26857–26864, September 2007.

[22] Simmie L. Foster, Diana C. Hargreaves, and Ruslan Medzhitov. Gene-specific control of inflammation by TLR-induced chromatin modifications. *Nature*, 447(7147):972–978, June 2007.

[23] Hnin Thanda Aung, Kate Schroder, Stewart R. Himes, Kristian Brion, Wendy Van Zuylen, Angela Trieu, Harukazu Suzuki, Yoshihide Hayashizaki, David A. Hume, Matthew J. Sweet, and Timothy Ravasi. LPS regulates proinflammatory gene expression in macrophages by altering histone deacetylase expression. *The FASEB Journal*, 20(9):1315–1327, 2006.

[24] Jörg Mages, Harald Dietrich, and Roland Lang. A genome-wide analysis of LPS tolerance in macrophages. *Immunobiology*, 212(9-10):723–737, January 2008.

[25] Tao Yang, Feipeng Zhang, Galip Gürkan Yardımcı, Fan Song, Ross C Hardison, William Stafford, Feng Yue, and Qunhua Li. HiCRep: Assessing the reproducibility of Hi-C data using a stratum-adjusted correlation coefficient. page 37.

[26] John J. Seeley and Sankar Ghosh. Molecular mechanisms of innate memory and tolerance to LPS. *Journal of Leukocyte Biology*, 101(1):107–119, January 2017.

[27] Uku Raudvere, Liis Kolberg, Ivan Kuzmin, Tambet Arak, Priit Adler, Hedi Peterson, and Jaak Vilo. G:Profiler: A web server for functional enrichment analysis and conversions of gene lists (2019 update). *Nucleic Acids Research*, 47(W1):W191–W198, July 2019.

[28] Daniele Merico, Ruth Isserlin, Oliver Stueker, Andrew Emili, and Gary D. Bader. Enrichment Map: A Network-Based Method for Gene-Set Enrichment Visualization and Interpretation. *PLOS ONE*, 5(11):e13984, November 2010.

[29] Laurel E. Hind, Emily B. Lurier, Micah Dembo, Kara L. Spiller, and Daniel A. Hammer. Effect of M1–M2 Polarization on the Motility and Traction Stresses of Primary Human Macrophages. *Cellular and Molecular Bioengineering*, 9(3):455–465, September 2016.

[30] E.V. Volpi, E. Chevret, T. Jones, R. Vatcheva, J. Williamson, S. Beck, R.D. Campbell, M. Goldsworthy, S.H. Powis, J. Ragoussis, J. Trowsdale, and D. Sheer. Large-scale chromatin organization of the major histocompatibility complex and other regions of human chromosome 6 and its response to interferon in interphase nuclei. *Journal of Cell Science*, 113(9):1565–1576, May 2000.

[31] Cyril Matthey-Doret, Lyam Baudry, Amaury Bignaud, Axel Cournac, Remi Montagne, Nadège Guiglielmoni, Foutel-Rodier Théo, and Scolari Vittore F. Simple library/pipeline to generate and handle Hi-C data. https://github.com/koszullab/hicstuff, March 2021.

[32] Nezar Abdennur and Leonid A Mirny. Cooler: Scalable storage for Hi-C data and other genomically labeled arrays. *Bioinformatics*, 36(1):311–316, January 2020.

[33] Open2c/cooltools. Open Chromosome Collective, April 2021.

[34] Cyril Matthey-Doret, Lyam Baudry, Axel Breuer, Rémi Montagne, Nadège Guiglielmoni, Vittore Scolari, Etienne Jean, Arnaud Campeas, Philippe Henri Chanut, Edgar Oriol, Adrien Méot, Laurent Politis, Antoine Vigouroux, Pierrick Moreau, Romain Koszul, and Axel Cournac. Computer vision for pattern detection in chromosome contact maps. *Nature Communications*, 11(1):5795, November 2020.

[35] Cyril Matthey-Doret. Koszullab/pareidolia: V0.6.1. https://zenodo.org/record/5062485, July 2021.

[36] Zhuoqing Fang. Gseapy: Gene Set Enrichment Analysis in Python.

[37] Aaron R. Quinlan and Ira M. Hall. BEDTools: A flexible suite of utilities for comparing genomic features. *Bioinformatics*, 26(6):841–842, March 2010.

a

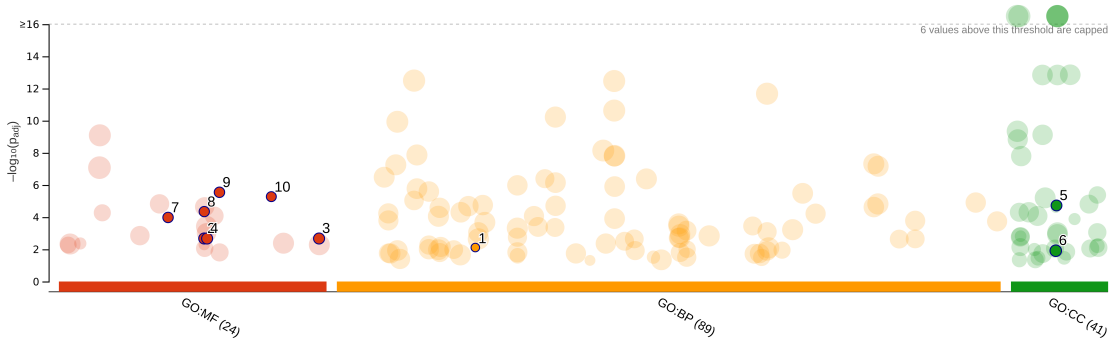

ID	Source	Term ID	Term Name	p_{adj} (query_1)
1	GO:BP	GO:0018916	nitrobenzene metabolic process	7.730×10^{-3}
2	GO:MF	GO:0042608	T cell receptor binding	2.119×10^{-3}
3	GO:MF	GO:1900750	oligopeptide binding	2.119×10^{-3}
4	GO:MF	GO:0043295	glutathione binding	2.119×10^{-3}
5	GO:CC	GO:0042824	MHC class I peptide loading complex	1.871×10^{-5}
6	GO:CC	GO:0042611	MHC protein complex	1.222×10^{-2}
7	GO:MF	GO:0030881	beta-2-microglobulin binding	1.040×10^{-4}
8	GO:MF	GO:0042610	CD8 receptor binding	4.500×10^{-5}
9	GO:MF	GO:0046977	TAP binding	2.834×10^{-6}
10	GO:MF	GO:0062061	TAP complex binding	5.291×10^{-6}

b

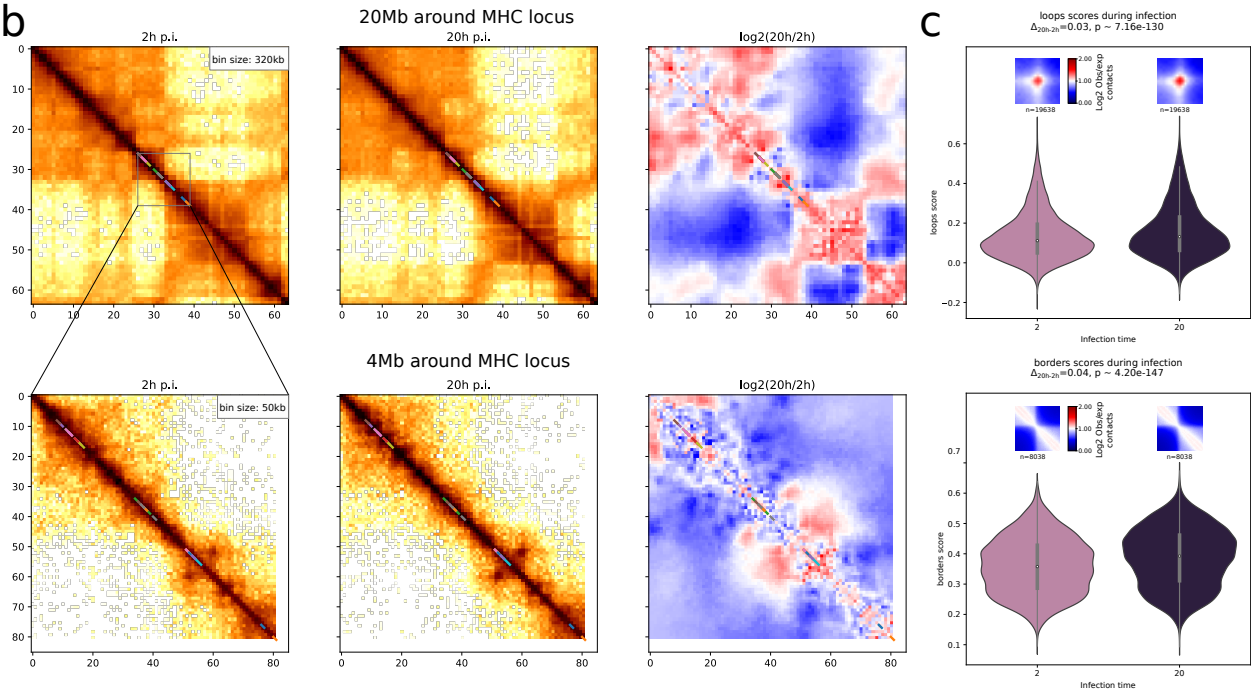

c

Figure 2: Hi-C changes during late infection. **a,** Overrepresentation analysis analysis of gene ontology terms in CHESS-positive regions showing structural changes during infection. The top 10 terms with highest enrichment odds ratio are highlighted. Point size represent the number of genes constituting a GO term, and the vertical position represents the p-value from Fisher exact test adjusted for multiple testing using g:profiler's SCS algorithm [27]. **b,** Hi-C contacts around the MHC locus at low (top) and medium (bottom) resolutions. Contacts are shown during early (left) and late (middle) infection. The serpentine-binned ratio showing contact changes during infection is shown on the right. **c,** Distribution of loops (top) and borders (bottom) intensity at early and late infection. Pileup plots show the average 2D profile of patterns in each condition. P-values are computed using Wilcoxon's signed-rank test.

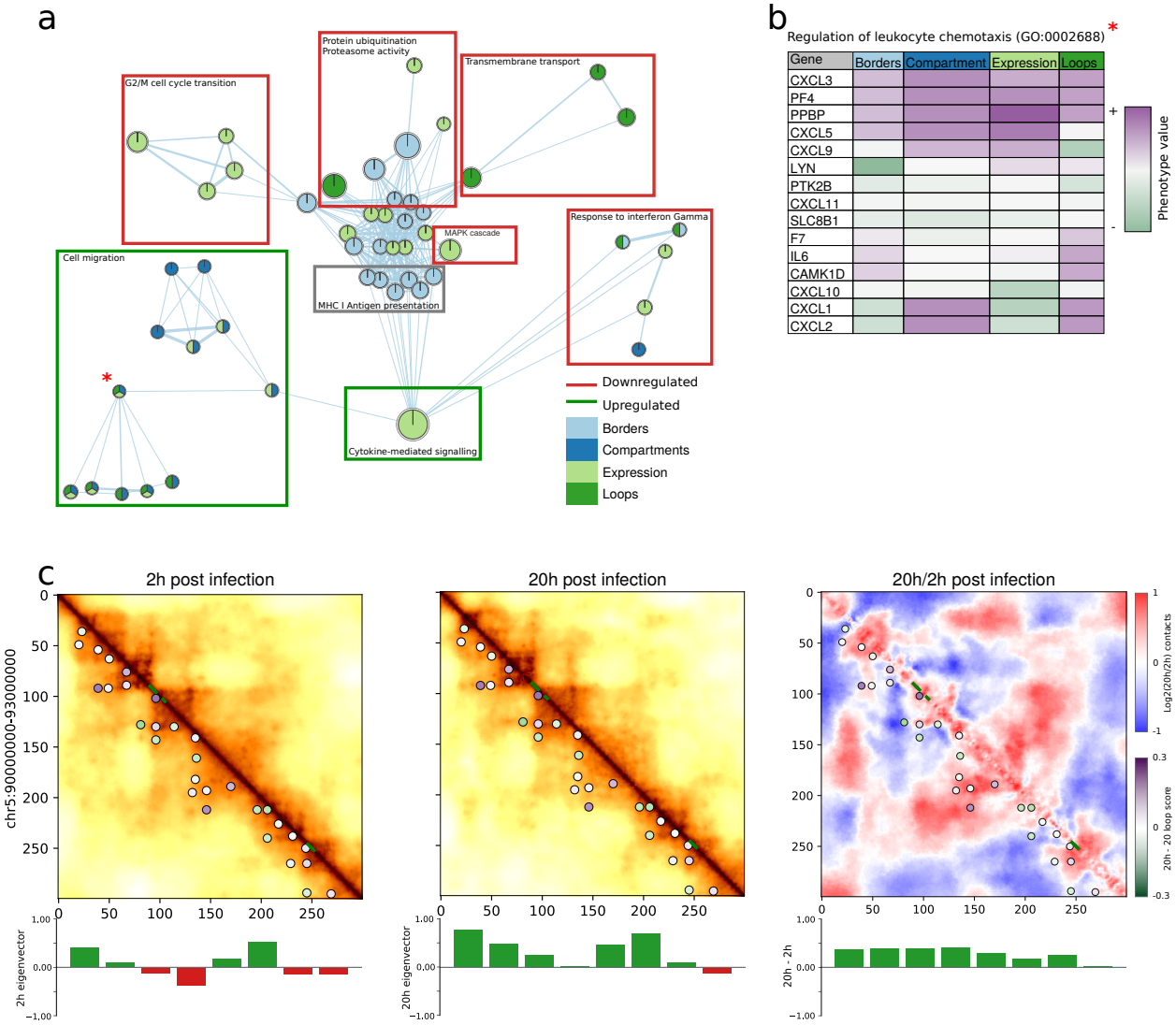

Figure 3: Gene set enrichment analysis of chromatin features. **a,** Largest connected component of the GSEA graph from chromatin features and gene expression change during infection. Each node is a GO:BP term, edges represent the proportion of gene overlap between terms (minimum cutoff 37.5%). Nodes are colored according to the feature (expression, compartment, border or loop change) in which they are significantly enriched during late infection (20h vs 2h). Functional subregions of the graph have been manually annotated, and the frame is colored based on its gene expression change (red: significantly downregulated, green: significantly upregulated, grey: neutral). **b,** Feature enrichment for genes involved in the GO term "Regulation of leukocyte chemotaxis", denoted by a red star on the graph. **c,** Hi-C contacts in the region containing chemokine genes CXCL3 and CXCL5. Chemokine genes are highlighted in green along the main diagonal. All matrices were binned at 10kb resolution and smoothed using Serpentine adaptive binning.

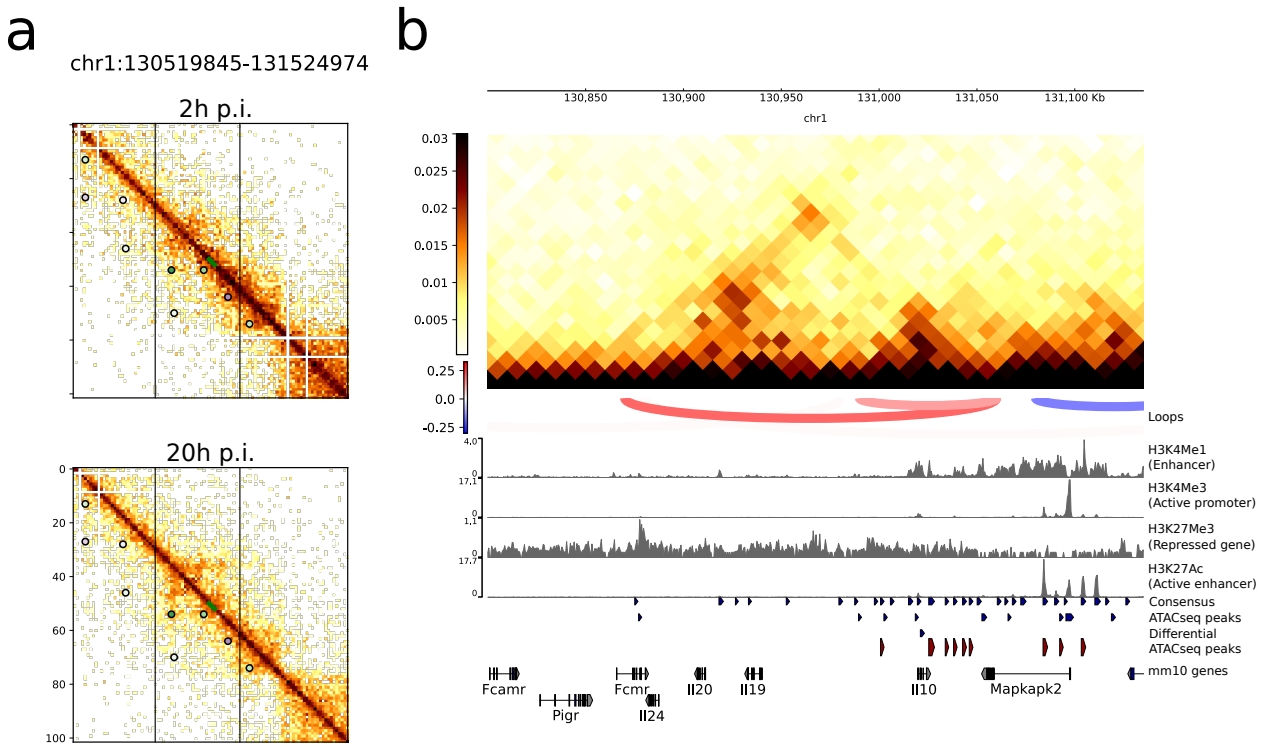

Figure 4: Epigenetic landscape around IL-10. A chromatin loop anchored next to the Il10 gene appears at 20h p.i. (top). The right anchor falls into a region with enhancer epigenetic marks. The left anchor falls close to Il24 and is rich in repressive marks.

4 Supplementary figures

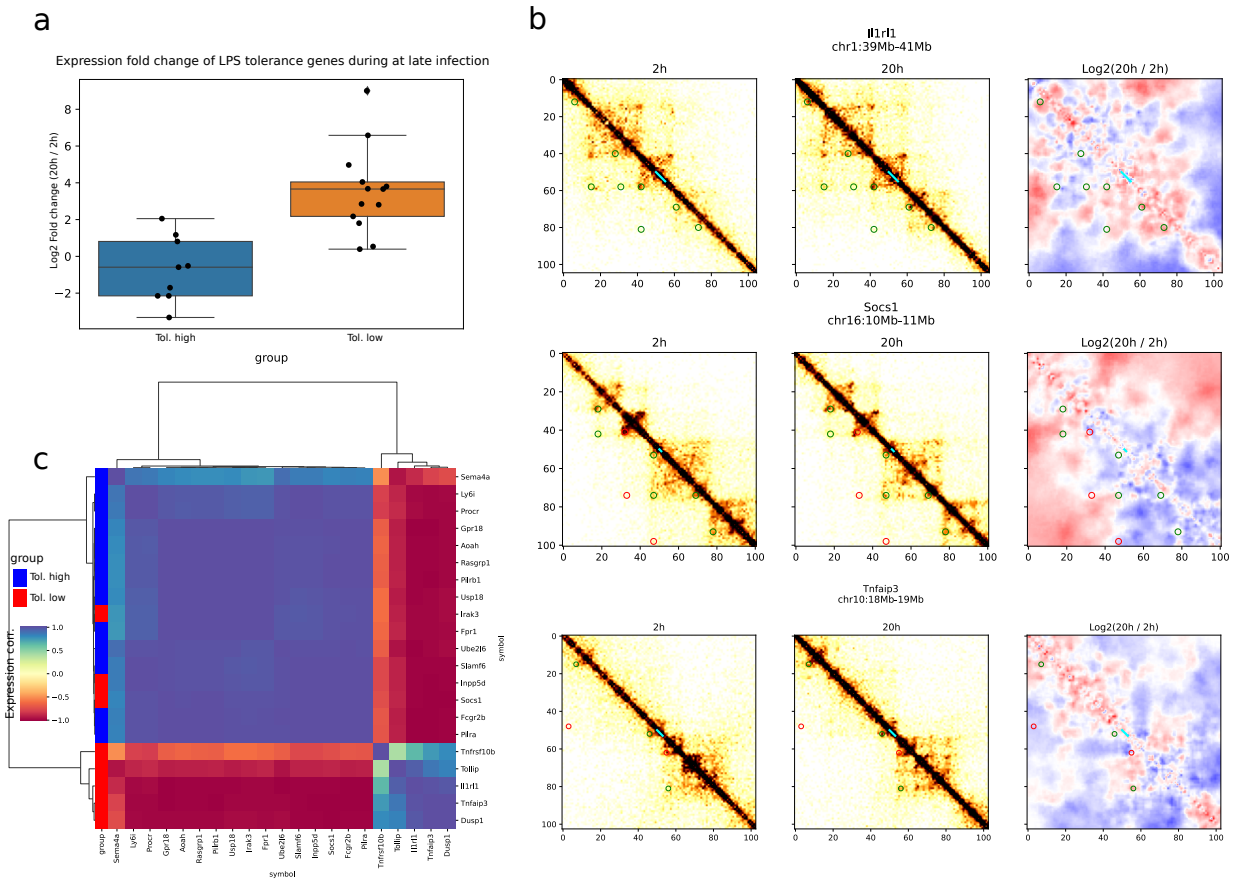

Figure S1: Analysis of select LPS marker genes from [24]. **a,** Expression of 22 genes known to be upregulated (Tol. up) and downregulated (Tol. low) during LPS tolerance, in our RNAseq results. **b,** Example Hi-C regions from genes with strong loop changes. Contacts at early (2h, left) late (20h, middle) and change during late infection (20h/2h, right) are shown. All matrices were binned at 10kb and ratios are smoothed using Serpentine adaptive binning. **c,** Gene expression correlation between LPS marker genes. Pearson correlation across all 4 samples is shown (duplicates at 2h and 20h).

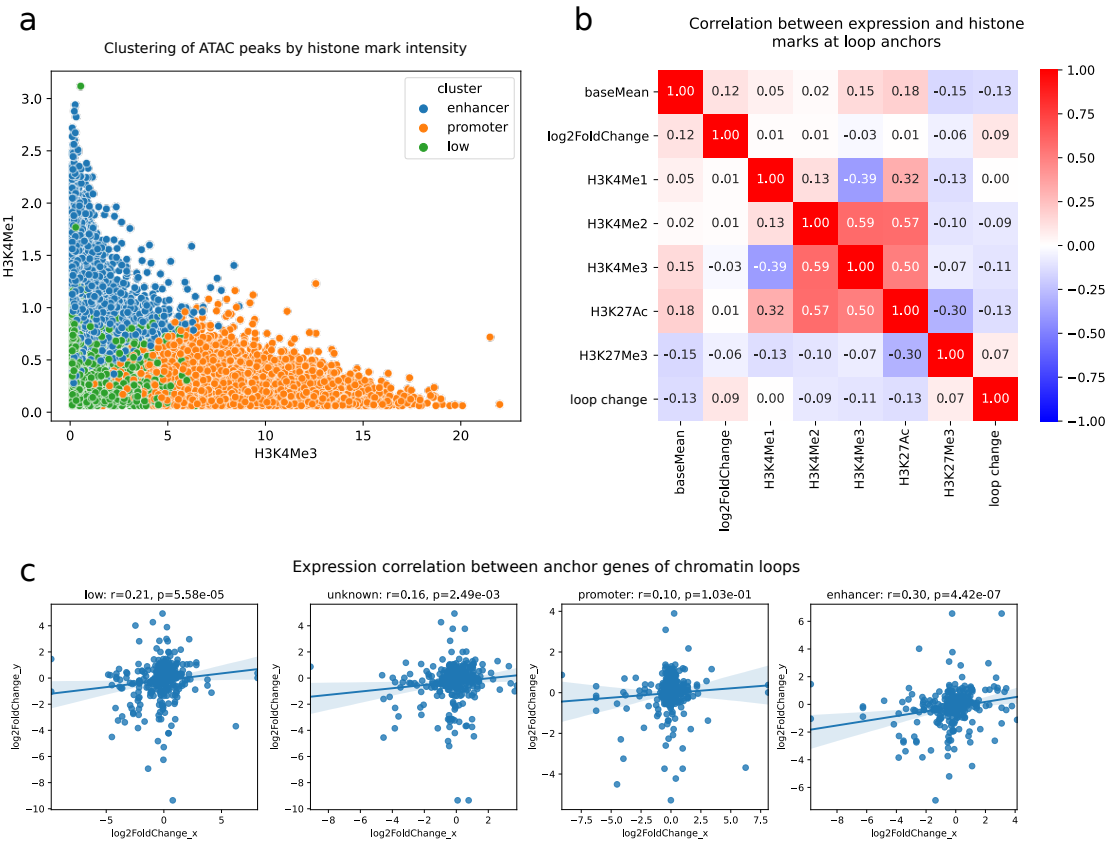

Figure S2: Analysis of epigenetic marks at loop anchors. **a,** Distribution of ATACseq peaks based on histone mark intensities H3K4Me3 and H3K4Me1. Colors represent cluster value assigned on the basis of 5 histone marks (H3K4Me1, H3K4Me2, H3K4Me3, H3K27Ac, H3K27Me3). **b,** Correlation between base gene expression (baseMean), gene expression fold change during infection (log2FoldChange), histone marks and loop intensity change during infection (loop change) at loop anchors. **c,** Expression correlation between gene pairs at loop anchors based on loop categories. Loop categories are defined as either anchor containing a histone mark-derived annotation.